

# Polygamain, a New Microtubule Depolymerizing Agent That Occupies a Unique Pharmacophore in the Colchicine Site<sup>§</sup>

R. M. Hartley, J. Peng, G. A. Fest, S. Dakshanamurthy, D. E. Frantz, M. L. Brown, and S. L. Mooberry

Departments of Pharmacology (R.M.H., J.P., G.A.F., S.L.M.) and Medicine (S.L.M.) and Cancer Therapy & Research Center (J.P., D.E.F., S.L.M.), University of Texas Health Science Center at San Antonio, San Antonio, Texas; Drug Discovery Program, Georgetown University Medical Center, Washington DC (S.D., M.L.B.); and Department of Chemistry, University of Texas at San Antonio, San Antonio, Texas (D.E.F.)

Received September 16, 2011; accepted December 14, 2011

## ABSTRACT

Bioassay-guided fractionation was used to isolate the lignan polygamain as the microtubule-active constituent in the crude extract of the Mountain torchwood, *Amyris madrensis*. Similar to the effects of the crude plant extract, polygamain caused dose-dependent loss of cellular microtubules and the formation of aberrant mitotic spindles that led to G<sub>2</sub>/M arrest. Polygamain has potent antiproliferative activities against a wide range of cancer cell lines, with an average IC<sub>50</sub> of 52.7 nM. Clonogenic studies indicate that polygamain effectively inhibits PC-3 colony formation and has excellent cellular persistence after wash-out. In addition, polygamain is able to circumvent two clinically relevant mechanisms of drug resistance, the expression of P-glycoprotein and the  $\beta$ III isotype of tubulin. Studies with purified tubulin show that polygamain inhibits the rate and

extent of purified tubulin assembly and displaces colchicine, indicating a direct interaction of polygamain within the colchicine binding site on tubulin. Polygamain has structural similarities to podophyllotoxin, and molecular modeling simulations were conducted to identify the potential orientations of these compounds within the colchicine binding site. These studies suggest that the benzodioxole group of polygamain occupies space similar to the trimethoxyphenyl group of podophyllotoxin but with distinct interactions within the hydrophobic pocket. Our results identify polygamain as a new microtubule destabilizer that seems to occupy a unique pharmacophore within the colchicine site of tubulin. This new pharmacophore will be used to design new colchicine site compounds that might provide advantages over the current agents.

## Introduction

Microtubule-disrupting agents have found excellent utility in the treatment of adult and pediatric cancers, and new drugs with improved properties continue to achieve FDA approval for cancer treatment. Drugs that target cellular microtubules can be divided into two groups, microtubule stabilizers and microtubule destabilizers, on the basis of their effects on tubulin polymerization and cellular microtu-

bules. Microtubule-stabilizing agents promote tubulin assembly and increase the density of cellular microtubules, whereas microtubule depolymerizers inhibit tubulin assembly and cause loss of cellular microtubules. The taxanes and epothilones are clinically useful microtubule stabilizers, and the microtubule depolymerizing vinca alkaloids also have clinical utility. Colchicine is a microtubule depolymerizer that binds to tubulin at a site distinct from that of the vinca alkaloids. Although colchicine has not proven to be useful in the treatment of cancer, multiple compounds that bind within the colchicine site, including combretastatin A (CA)-4 phosphate, are advancing in clinical trials for anticancer indications.

The identification of new drugs that can circumvent drug resistance is critically important to advance cancer therapeutics. Some tumors are intrinsically resistant to chemotherapy, and others develop resistance after therapy. Multiple mechanisms of drug resistance have been identified for microtubule-targeting agents, including expression of ATP-

This work was supported by the Department of Defense Prostate Program [Grant W81XWH-08-1-0395]; the National Institutes of Health National Institute of Dental and Craniofacial Research COSTAR Program [Grant T32-DE14318]; and the National Institutes of Health National Cancer Institute [Grant P30-CA054174] (to the Cancer Therapy & Research Center at the University of Texas Health Science Center at San Antonio). We acknowledge the use of the CTRC Flow Cytometry and Macromolecular Structure shared resources.

Article, publication date, and citation information can be found at <http://molpharm.aspetjournals.org>.

<http://dx.doi.org/10.1124/mol.111.075838>.

<sup>§</sup> The online version of this article (available at <http://molpharm.aspetjournals.org>) contains supplemental material.

**ABBREVIATIONS:** CA, combretastatin; FBS, fetal bovine serum; Pgp, P-glycoprotein; DMSO, dimethyl sulfoxide; WT, wild-type;  $\beta$ III,  $\beta$ III tubulin; Rr, relative resistance.

binding cassette transporters that limit cellular drug accumulation. Expression of the *mdr-1* gene product P-glycoprotein (Pgp) leads to diminished intracellular drug accumulation and to attenuated cytotoxic effects in vitro and in vivo (Gottesman et al., 2002). The expression of Pgp in both hematological and solid tumors is associated with poor treatment response to a number of drugs (Yeh et al., 2003; Penson et al., 2004). All tubulin-binding anticancer drugs used clinically except cabazitaxel are substrates for Pgp, thus limiting their activity in multidrug-resistant tumors.

In addition, multiple target-based resistance mechanisms, including alterations in  $\beta$ -tubulin, are linked with clinical drug resistance (Dumontet and Jordan, 2010; Kavallaris, 2010). Mammals have seven  $\beta$ -tubulin genes, resulting in tubulin isotypes that are highly homologous but differ primarily in the 10 to 15 amino acids of the carboxyl terminus (Ludueña, 1998). In cell lines, overexpression of  $\beta$ III tubulin is associated with resistance to tubulin binding antimetabolic agents (Kavallaris, 2010). Expression of the  $\beta$ III tubulin isotype in ovarian cancer, non-small-cell lung cancer, and breast cancer is linked with resistance to the taxanes (Galmarini et al., 2008; Dumontet et al., 2009; Sève et al., 2010). Although many mechanisms of resistance to microtubule-targeting agents have been identified in cell lines (Kavallaris, 2010), only expression of Pgp or the  $\beta$ III tubulin isotype have been linked with clinical resistance. The identification of new microtubule-targeting agents that can overcome multidrug resistance mechanisms will provide a major advance.

Our laboratory has expertise in the identification of new microtubule-binding agents from diverse natural products, including cyanobacteria (Smith et al., 1994), sponges (Mooberry et al., 1999), and tropical plants (Tinley et al., 2003b). Plants historically have been an excellent source for microtubule-disrupting drugs; paclitaxel (Taxol) was first isolated from the bark of the Pacific yew, *Taxus brevifolia* (Wani et al., 1971); the vinca alkaloids were isolated from the Madagascar periwinkle (Noble et al., 1958); and colchicine was isolated from the autumn crocus (Eigsti and Dustin, 1955). Colchicine binds to a distinct drug binding site on tubulin; however, it is too toxic for use as an anticancer agent. Another plant-derived microtubule depolymerizer that binds to the colchicine site, podophyllotoxin, was first isolated from the Mayapple, *Podophyllum peltatum* (Podwysotski, 1880), and although it was effective against skin cancers, it was also too toxic for systemic use. The combretastatins are colchicine site-binding drugs that were initially isolated from the African bush willow, *Combretum caffrum* (Pettit et al., 1987). Combretastatin A4 phosphate [fosbretabulin (Zybrestat)] is advancing in clinical trials, suggesting that the colchicine site on tubulin has potential as an anticancer drug target. We hypothesized that new microtubule active compounds could continue to be identified from nature, and a project was initiated to evaluate the chemistry of plants that thrive in the harsh environment of south Texas for microtubule-interacting compounds. One thousand eighty-eight extracts were made from 368 Texas plants, and the extracts were evaluated for effects on the cytoskeleton and for cytotoxicity against a panel of cancer cell lines. One extract had potent microtubule-depolymerizing properties, and we identified the active constituent as polygamain, a cytotoxic compound with a previously unknown mechanism of action. Here we describe the

molecular pharmacology of this new tubulin-binding microtubule-depolymerizing agent.

## Materials and Methods

**Isolation of Polygamain from *Amyris madrensis*.** The leaves and stems of *A. madrensis*, the Mountain torchwood, were collected, frozen, and lyophilized. The freeze-dried material was ground to a powder and extracted using supercritical CO<sub>2</sub>. The crude extract was tested in a cell-based phenotypic screen for effects on cellular microtubules, and microtubule depolymerization was observed. Bioassay-guided fractionation using silica gel flash chromatography and C18 high-performance liquid chromatography was used to isolate the active constituent. The structure of polygamain was determined using one- and two-dimensional NMR as well as mass spectroscopic methods. The data were compared with those reported previously (Hokanson, 1979; Sheriha et al., 1987).

**Structure Elucidation.** The structure of polygamain was determined using the following data (polygamain): ESIMS *m/z*: 353.1 [M + H], 335 [M + H - H<sub>2</sub>O]; <sup>1</sup>H NMR (CDCl<sub>3</sub>)  $\delta$  (parts per million) 2.27 (m, H-2), 2.75 (m, H-3), 2.76 (m, H $\alpha$ -4), 3.06 (d, *J* = 10.8 Hz, H $\beta$ -4), 3.91 (t, *J* = 8.2 Hz, H $\beta$ -11), 4.44 (dd, *J* = 8.0 Hz, 5.4, H $\alpha$ -11), 4.56 (d, *J* = 4.1 Hz, H-1), 5.89 (s, 6,7-OCH<sub>2</sub>O-), 5.90 (s, 6,7-OCH<sub>2</sub>O-), 5.92 (s, 3',4'-OCH<sub>2</sub>O-), 6.47 (s, H-8), 6.60 (s, H-2'), 6.62 (d, *J* = 8.1 Hz, H-6'), 6.65 (s, H-5), and 6.68 (d, *J* = 7.7 Hz, H-').

**Materials.** Podophyllotoxin was purchased from Sigma-Aldrich (St. Louis, MO). The potassium salt of CA-4 was synthesized by the Frantz laboratory using a method based on those reported by Pettit et al. (1995).

**Cell Culture.** A549, SCC-4, HeLa, SK-OV-3, A-10, PC-3, and DU 145 cells were purchased from the American Type Culture Collection (Manassas, VA). Prostate epithelial cells were purchased from Lonza Walkersville, Inc. (Walkersville, MD). MDA-MB-435 and MDA-MB-231 cells were obtained from the Lombardi Cancer Center, Georgetown University (Washington DC). A549, MDA-MB-231, MDA-MB-435, and DU 145 cell lines were grown in modified improved minimum essential medium (Invitrogen, Carlsbad, CA) with 10% fetal bovine serum (FBS) and 25  $\mu$ g/ml gentamicin. A-10 and HeLa cells were cultured in basal medium Eagle with Earle's salts (Sigma-Aldrich) with 10% FBS and 50  $\mu$ g/ml gentamicin. SCC-4 cells were cultured in Dulbecco's modified Eagle's medium (Invitrogen) with 10% FBS and 50  $\mu$ g/ml gentamicin. PC-3 cells were grown in RPMI 1640 medium (Invitrogen) with 10% FBS and 50  $\mu$ g/ml gentamicin. Prostate epithelial cells were cultured in Prostate Epithelial Cell Basal Medium (Lonza Walkersville, Inc.). HeLa WT $\beta$ III and SK-OV-3-MDR-1-6/6 cell lines were obtained, characterized, and grown as described previously (Risinger et al., 2008). All experiments were conducted using cells in log phase growth.

**Indirect Immunofluorescence and EC<sub>50</sub> Calculation.** The effects of polygamain on cellular microtubules were evaluated in A-10 and HeLa cells by indirect immunofluorescence. Cells were treated with vehicle (DMSO) or drug for 18 h and fixed, and microtubules were visualized using a monoclonal anti- $\beta$ -tubulin antibody produced in mouse (clone TUB 2.1, ascites fluid; Sigma) as described previously (Tinley et al., 2003a). Cells were stained with 0.1  $\mu$ g/ml 4',6-diamidino-2-phenylindole to visualize DNA. Images were analyzed using a Nikon Eclipse 80i microscope (Nikon Instruments, Melville, NY) and NIS Elements Advanced Research imaging software (Nikon Instruments). The EC<sub>50</sub> (concentration required to cause 50% loss of cellular microtubules) was determined in A-10 cells as described previously (Lee et al., 2010) and represents the average from three independent experiments.

**Cell Cycle Analysis.** Cell cycle distribution of HeLa cells was determined by flow cytometry. Cells were treated with vehicle (DMSO) or drug for 18 h. The cells were harvested, stained with Krishan's reagent (Krishan, 1975), and analyzed with a FACSCalibur flow cytometer (BD Biosciences, San Jose, CA).

**Inhibition of Cellular Proliferation.** Inhibition of cellular proliferation was measured using the sulforhodamine B assay (Skehan et al., 1990; Boyd and Paull, 1995). Cells were plated in 96-well plates, allowed to attach and grow for 24 h, and then treated with vehicle or a range of drug concentrations for 48 h.  $IC_{50}$  values were calculated from at least three independent experiments, each conducted in triplicate as described previously, and are presented as the mean  $\pm$  S.D. (Tinley et al., 2003b).

**Clonogenic Assay.** PC-3 cells were plated at a density of 200 cells per 60-mm tissue culture dish; 24 h after plating, they were treated with vehicle (DMSO) or the  $IC_{50}$  concentration of each compound. After a 12-h exposure, the drug-containing media were removed, the cells were washed with warm sterile PBS, and fresh media were added to the plates. After an additional 9 days, the colonies were washed with PBS and stained with a 20% MeOH:0.5% crystal violet solution. Colonies were counted using GeneTools software (Syngene, Frederick, MD) in four independent experiments.

**Tubulin Assembly.** Purified porcine brain tubulin (Cytoskeleton, Denver, CO) was diluted to 3 mg/ml with tubulin buffer and incubated with 10% glycerol and 1 mM GTP in the presence of vehicle or drug. Tubulin polymerization was monitored by absorbance at 340 nm for 1 h at 37°C.

**Colchicine Displacement.** The ability of polygamain to displace colchicine binding to tubulin was evaluated using a fluorescent colchicine displacement assay (Das et al., 2009) as described previously (Risinger et al., 2011). In brief, a solution containing 2  $\mu$ M tubulin alone or 2  $\mu$ M colchicine and 2  $\mu$ M tubulin was incubated for 2 h at 37°C with vehicle or competing drug. The fluorescence of the samples was analyzed using a Horiba Fluoromax-3 spectrofluorometer (Horiba Jobin Yvon, Edison, NJ) using an excitation wavelength of 380 nm and an emission wavelength of 438 nm (Banerjee and Luedueña, 1992). The fluorescence values were normalized by subtracting the baseline of buffer alone and defining the fluorescence of tubulin and colchicine as 100%.

**Molecular Modeling and Docking Studies.** The X-ray crystal structure of two  $\alpha\beta$ -tubulin heterodimers complexed with podophyllotoxin fragment (Protein Data Bank code 1SA1) was used for the molecular docking simulations of polygamain. Tubulin structure was minimized with AMBER 9.0 (<http://ambermd.org/>) with SANDER default parameters. Docking experiments were performed using SurflexDock module of Sybyl 8.1 (Tripos International, St. Louis, MO) with the number of solution conformations set to 90. The best docked geometry for polygamain was energy-minimized with the SANDER module of AMBER 9.0.

**Molecular Dynamics Simulations.** The minimized complex was subjected to molecular dynamics simulations using AMBER 9.0 with the general amber force field (Wang et al., 2004) and root-mean-square deviation charge models (Bayly et al., 1993). Molecular dynamics simulations performed in the NVE (number of atoms/volume/energy) ensemble consisted of an initial equilibration of 25 ps followed by a production run of 300-ps dynamics at 300 K. The final complex structure at the end of the molecular dynamics simulation was subjected to 2000 steps of steepest descent energy minimization followed by conjugate gradient energy minimization. A distance-dependent dielectric constant and nonbonded distance cutoff of 12 Å were used.

**Aqueous Solubility.** The aqueous solubility of polygamain was determined using a protocol modified from the Millipore solubility assay as described previously (Lee et al., 2010). A standard curve was generated using fixed concentrations of each drug in a universal solvent. The concentration of each drug in an aqueous solution was determined from the standard curve using linear regression. Values are an average of two independent experiments.

**Statistical Analysis.** Data are reported as mean  $\pm$  S.D. The statistical significance of the data from the clonogenic assays was determined using a one-tailed Student's *t* test. Differences were considered significant at  $p < 0.05$ .

## Results

**Isolation of Polygamain and Evaluation of its Microtubule and Cell Cycle Effects.** Potent microtubule depolymerizing activity was observed in a lipophilic extract of *A. madrensis*. Bioassay-guided fractionation yielded polygamain (Fig. 1A) as the microtubule-active constituent. Polygamain is structurally similar to podophyllotoxin (Fig. 1B), a known cytotoxic lignan with microtubule-depolymerizing activity. Polygamain and podophyllotoxin are both lignans and represent a different structural class than the well-known microtubule depolymerizers colchicine and CA-4 (Fig. 1, C and D).

The effects of polygamain on cellular microtubules were evaluated in A-10 and HeLa cells and compared with the effects initiated by podophyllotoxin or CA-4. A-10 cells are useful for evaluating microtubule-disrupting agents because they are large, flat and, like other smooth muscle cells, they arrest in interphase in response to tubulin-binding agents (Blagosklonny et al., 2004). Normal interphase microtubules form an intricate network that extends from the microtubule-organizing center in the central region of the cell and radiates out to the cell membrane (Fig. 2A). Polygamain caused a concentration-dependent loss of cellular microtubules. The first effect noticed was a loss of microtubules in the cell periphery with a 75 nM concentration. Higher concentrations of polygamain caused more extensive microtubule loss, and total depolymerization occurred with 1  $\mu$ M (Fig. 2C). The effects of a 290 nM concentration are shown in Fig. 2B, and they were essentially identical to the microtubule-depolymerizing effects initiated by podophyllotoxin or CA-4, but polygamain was substantially less potent. Initial microtubule depolymerization was observed with 3.5 nM podophyllotoxin, and total depolymerization occurred with 10 nM podophyllotoxin (Supplemental Fig. 1A). CA-4 at 5 nM caused modest microtubule loss, and total depolymerization was seen with a 20 nM concentration (Supplemental Fig. 1B). Polygamain has an  $EC_{50}$ , the concentration that causes approximately 50% loss of cellular microtubules of 290 nM. In comparison, the  $EC_{50}$  for podophyllotoxin and CA-4 were 6

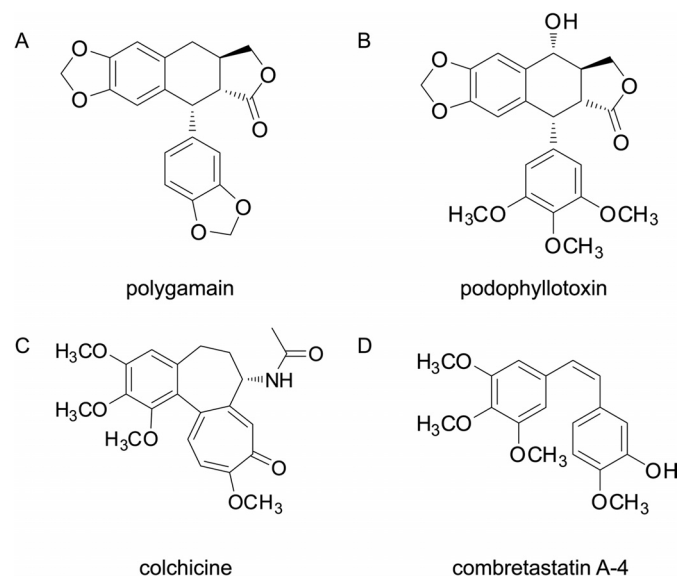


**Fig. 1.** Chemical structures of polygamain (A), podophyllotoxin (B), colchicine (C), and combretastatin A-4 (D).

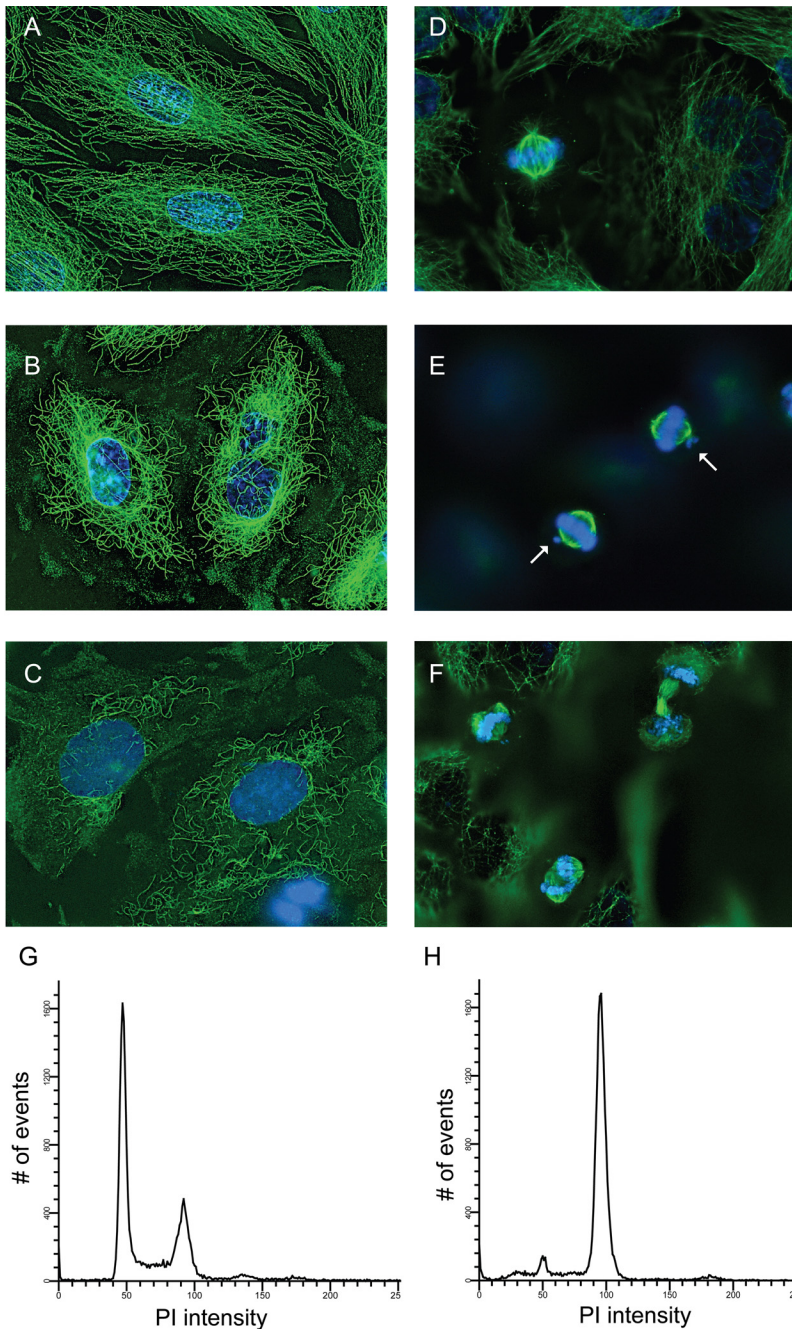


**Fig. 2.** Effects of polygamain on interphase microtubules, mitotic spindles and cell cycle distribution. A-10 cells treated with vehicle (DMSO) (A), 290 nM polygamain (B), or 1  $\mu$ M polygamain (C). HeLa cells were treated with vehicle (D), 20 nM polygamain (E), or 50 nM polygamain (F). Cellular microtubules were visualized using indirect immunofluorescence. HeLa cells were treated with vehicle (G) or 50 nM polygamain (H) for 18 h and stained with Krishan's reagent, and cell cycle distribution quantified using flow cytometry.

and 10 nM, respectively (Supplemental Fig. 1, C and D). Podophyllotoxin and CA-4 showed very steep dose response curves in this assay, whereas polygamain's effects occurred over a much broader range, yielding a substantially higher  $EC_{50}$ .

The effects of polygamain on mitotic spindles were evaluated in HeLa cells. Normal bipolar mitotic spindles and chromatin congression at the metaphase plate was observed in vehicle-treated cells (Fig. 2D). No effects on either mitotic spindles or DNA alignment was noted with a 10 nM concentration of polygamain, but with 20 nM, lagging chromosomes at one or both spindle poles were observed, even though phenotypically normal bipolar mitotic spindles were present (Fig. 2E). With higher concentrations, 25 and 30 nM polygamain, multiple mitotic defects were noted, including lack of

complete DNA congression at the metaphase plate and the formation of multipolar mitotic spindles (data not shown). A 50 nM concentration of polygamain caused the formation of multiple mitotic spindle asters in mitotic cells, accompanied by failure of DNA congression at the metaphase plate (Fig. 2F), suggesting that the mitotic spindles were unable to function normally. Multipolar mitotic spindles were retained with higher concentrations of polygamain, but the length of the spindles diminished, and very short spindles radiated from the spindle asters. Similar effects are seen with podophyllotoxin and CA-4 (Supplemental Fig. 1, E and F) and have been noted with other microtubule depolymerizers (Tingley et al., 2003a; Risinger et al., 2011).

These results indicate that polygamain interrupts the ability of the mitotic spindles to align the chromosomes in the

metaphase plate and suggests that it interrupts cell division. This was tested by evaluating the effects of polygamain on cell cycle progression. HeLa cells were treated with polygamain, podophyllotoxin, or CA-4 to determine the lowest concentration that caused maximal G<sub>2</sub>/M accumulation. Although vehicle-treated cells had a normal cell cycle distribution (Fig. 2G), each of the microtubule-disrupting agents caused dose-dependent G<sub>2</sub>/M accumulation. Maximal G<sub>2</sub>/M accumulation was achieved with 50 nM polygamain (Fig. 2H), 10 nM podophyllotoxin, and 10 nM CA-4 (data not shown).

**Polygamain Has Antiproliferative Activity against a Broad Range of Cancer Cell Lines.** The antiproliferative and cytotoxic effects of polygamain were evaluated using the sulforhodamine B assay in a panel of cancer cell lines (Table 1). Polygamain caused dose-dependent inhibition of proliferation in each of the cell lines with a mean IC<sub>50</sub> of 52.7 nM. In all the cell lines except A549 and MDA-MB-231, polygamain caused complete inhibition of cellular proliferation and initiated cell death. The A549 and MDA-MB-231 cell lines are known to be relatively resistant to anticancer agents (Huang et al., 2009), and in these cell lines, polygamain had only cytostatic effects, consistent with the effects of podophyllotoxin and CA-4 in these two cell lines. Podophyllotoxin has a low therapeutic window; therefore, the effects of polygamain and CA-4 were compared with the effects of podophyllotoxin in normal prostate epithelial cells. Each compound was evaluated at five times the average IC<sub>50</sub> concentration obtained in the cancer cell lines (as determined from Table 1). As expected, podophyllotoxin caused 42 ± 8% cell death of the normal cells. In contrast, polygamain caused only 5 ± 4% cell death, and 9 ± 2% cell death was observed with CA-4. Polygamain and CA-4 differ substantially from podophyllotoxin in their effects on normal epithelial cells.

**βIII-Mediated Drug Resistance.** The identification of new microtubule-targeting agents that can circumvent clinically relevant mechanisms of drug resistance could provide a major advance in cancer chemotherapy. One mechanism of drug resistance to microtubule-targeted agents is expression of the βIII isotype of tubulin. This tubulin isotype is normally found primarily in the brain (Ludueña and Banerjee, 2008); when expressed in cancer cells, it confers resistance to multiple microtubule-targeted agents including paclitaxel (Risinger et al., 2008). The ability of polygamain to overcome βIII tubulin-mediated multidrug resistance was evaluated in a HeLa isogenic cell line pair (Risinger et al., 2008). HeLa cells and a HeLa cell line overexpressing wild-type βIII tubulin (WTβIII) were treated with polygamain, podophyllotoxin, or CA-4, and inhibition of proliferation was evaluated. Poly-

gamain had an IC<sub>50</sub> of 36.9 nM in the WTβIII cell line and 37.9 nM in the parental HeLa cells (Table 1). A relative resistance value (Rr) was calculated by dividing the IC<sub>50</sub> obtained in the βIII-expressing cell line by the IC<sub>50</sub> value obtained in the parental cell line. A Rr value of 1.0 was calculated for polygamain, similar to the Rr of 1.1 obtained for podophyllotoxin and CA-4 (Table 1). These data indicate that the expression of βIII tubulin does not change the sensitivity of HeLa cells to these compounds, suggesting that they are able to overcome drug resistance mediated by the expression of βIII tubulin.

**Pgp-Mediated Drug Resistance.** Another major mechanism of multidrug resistance in cancer is expression of Pgp. An isogenic SK-OV-3 cell line pair was used to test the ability of polygamain to overcome Pgp-mediated drug resistance. The parental SK-OV-3 and the Pgp-expressing SK-OV-3-MDR-1-6/6 cell lines were treated with polygamain, podophyllotoxin, or CA-4, and the IC<sub>50</sub> values were determined (Table 1). Paclitaxel, a documented Pgp substrate, has an Rr value of 860 in this cell line pair, whereas non-Pgp substrates 2-methoxyestradiol and epothilone B have Rr values of 2.6 and 6.8, respectively (Risinger et al., 2008). The IC<sub>50</sub> values of polygamain were 51.3 and 102.1 nM, respectively, in the parental and Pgp-expressing cell lines, yielding an Rr of 2.0 (Table 1). This Rr value was slightly lower than but generally comparable with the 6.3 and 7.4 Rr values obtained for podophyllotoxin and CA-4 (Table 1). A direct drug efflux assay was also used to determine whether polygamain is a direct substrate of Pgp. Polygamain, podophyllotoxin, and CA-4 were unable to inhibit efflux of rhodamine 123, a fluorescent substrate of Pgp, but vinblastine, a known Pgp substrate, inhibited rhodamine 123 efflux (Supplemental Fig. 2). These data suggest that polygamain is a poor substrate for transport by Pgp and as such has advantages over many microtubule-targeted natural products.

**Polygamain Inhibits Colony Formation after a 12-h Drug Exposure.** A clonogenic assay was used to evaluate the ability of polygamain to inhibit colony formation of PC-3 cells after a 12-h exposure to the IC<sub>50</sub> concentration. Notable differences in cellular persistence have recently been noted among compounds representing diverse classes of microtubule-disrupting agents (Risinger and Mooberry, 2011; Towle et al., 2011). The effects of polygamain in this assay were compared with the effects of podophyllotoxin and CA-4. Representative plates are shown in Fig. 3A, and the number of colonies in each plate expressed as percentage of the vehicle-treated control. Differences in colony formation are apparent among these microtubule depolymerizers. Podophyllotoxin caused a slight (20%) inhibition of colony formation but CA-4

TABLE 1  
IC<sub>50</sub> values for antiproliferative activities of polygamain, podophyllotoxin, and CA-4 against diverse cancer cell lines

Cell Line	Polygamain IC <sub>50</sub>	Rr	Podophyllotoxin IC <sub>50</sub>	Rr	CA-4 IC <sub>50</sub>	Rr
	<i>nM</i>		<i>nM</i>		<i>nM</i>	
MDA-MB-435	26.3 ± 2.5		5.7 ± 0.5		2.4 ± 0.1	
DU 145	54.9 ± 4.6		9.4 ± 1.0		5.3 ± 0.3	
PC-3	70.6 ± 2.6		16.1 ± 1.3		7.9 ± 0.6	
SCC-4	36.4 ± 2.0		14.5 ± 0.5		7.3 ± 0.9	
A549	65.8 ± 3.7		9.8 ± 0.9		5.9 ± 0.5	
MDA-MB-231	78.2 ± 5.4		13.6 ± 1.0		7.3 ± 0.3	
HeLa	37.9 ± 1.9		8.4 ± 0.5		3.5 ± 0.4	
WTβIII	36.9 ± 1.5	1.0	9.1 ± 0.6	1.1	3.7 ± 0.8	1.1
SK-OV-3	51.3 ± 2.1		7.5 ± 0.2		4.4 ± 0.4	
SK-OV-3-MDR-1-6/6	102.1 ± 1.9	2.0	47.5 ± 2.5	6.3	32.4 ± 7.4	7.4

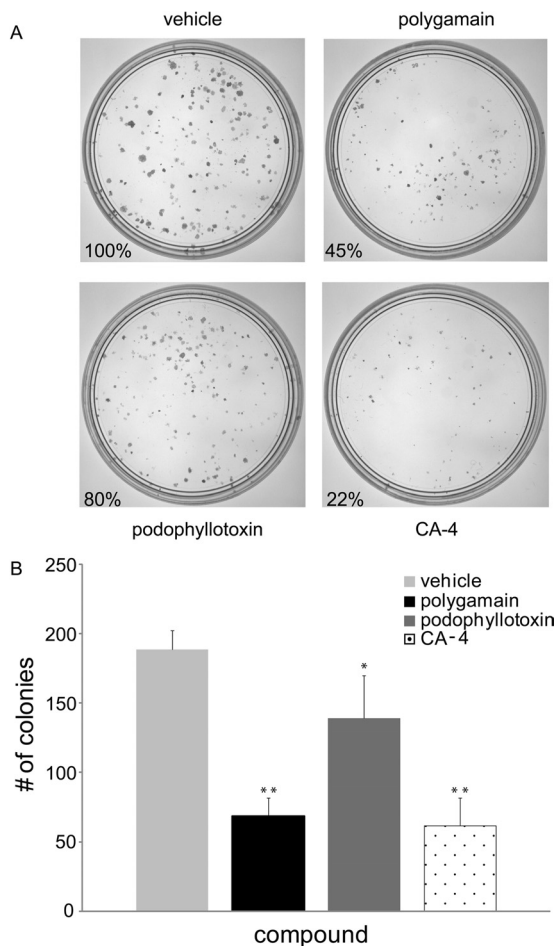


**Fig. 3.** Effects of a 12-h exposure on clonogenic cell viability. PC-3 cells were treated with the  $IC_{50}$  of polygamain, podophyllotoxin, or CA-4 for 12 h, then the media replaced. Colony formation is shown after an additional 9 days of growth (A). Quantification of the colony formation experiments ( $n = 3$ ) (B). Each compound inhibited colony formation to a statistically significant degree. \*\*,  $p < 0.05$ ; \*,  $p = 0.0$ .

was very effective, inhibiting colony formation by 88%. Polygamain was intermediate between these compounds, causing 55% inhibition of colony formation (Fig. 3A). The size of the resultant colonies was additionally affected, with the smallest colonies observed in the plates treated with CA-4 and the largest colonies in those treated with podophyllotoxin. At their respective  $IC_{50}$  values, polygamain and CA-4 were substantially more effective than podophyllotoxin at inhibiting colony formation after 12-h treatment, suggesting that polygamain and CA-4 have better cellular persistence than podophyllotoxin.

**Polygamain Inhibits Tubulin Assembly.** The microtubule-depolymerizing effects of polygamain suggested the possibility that it interacts directly with tubulin to inhibit assembly. This was tested using a biochemical tubulin polymerization assay. Polygamain inhibited the rate and overall extent of purified tubulin assembly in a concentration-dependent manner (Fig. 4A). A 1  $\mu$ M concentration of polygamain inhibited the extent of tubulin polymerization by 32% at 1 h. The rate of tubulin assembly can be determined by evaluating the time necessary to reach steady state, indicated by the plateau of the reaction (Fig. 4A). The plateau in the assembly reaction was reached after approximately 30 min in the vehicle control and yet even after 1 h, a plateau

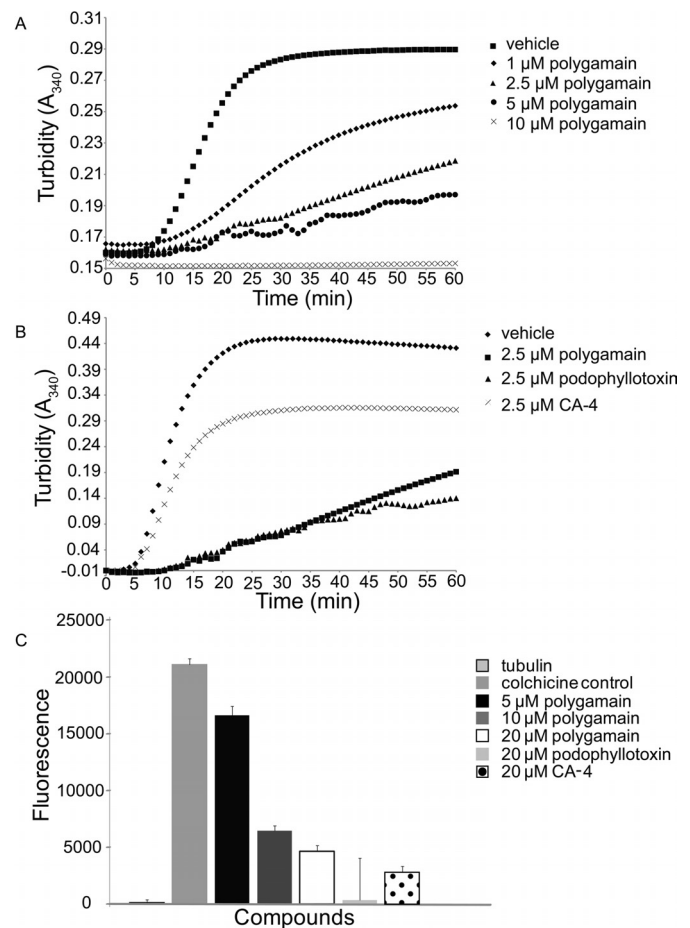


**Fig. 4.** Effects of polygamain on tubulin assembly and colchicine displacement. Tubulin polymerization in the presence of vehicle and a range of concentrations of polygamain (A). Tubulin polymerization in the presence of vehicle or 2.5  $\mu$ M polygamain, podophyllotoxin, or CA-4 (B). Controls from three different experiments were averaged and normalized to 1, and the individual data for each drug were normalized to control. Colchicine displacement by polygamain, podophyllotoxin, or CA-4 (C).

had not yet been reached with any concentration of polygamain tested. Total inhibition of tubulin polymerization was achieved with 10  $\mu$ M polygamain (Fig. 4A), and an  $IC_{50}$  for inhibition of tubulin assembly of 2.5  $\mu$ M was calculated. Podophyllotoxin and CA-4 also inhibited the rate and extent of tubulin polymerization in this assay with complete inhibition at 10  $\mu$ M, and  $IC_{50}$  values of 2.3 and 6.2  $\mu$ M, respectively. The effects of polygamain on tubulin assembly were essentially identical to those of CA-4 and podophyllotoxin, differing only in relative potency. At 2.5  $\mu$ M, podophyllotoxin inhibited tubulin polymerization by 64%, polygamain by 56%, and CA-4 by 29% (Fig. 4B). It is noteworthy that the rank potency of the three compounds in the purified tubulin assay is different from that obtained in the antiproliferative assays, where CA-4 was more potent than podophyllotoxin, and polygamain was the least potent in every cell line tested (Table 1).

**Polygamain Displaces Colchicine from Tubulin.** A colchicine displacement assay was used to evaluate the ability of polygamain to inhibit colchicine binding to tubulin. Although tubulin and colchicine are not fluorescent alone, colchicine binding to tubulin initiates a conformational change in colchicine, causing it to fluoresce (Bhattacharyya

and Wolff, 1974) (Fig. 4C). When colchicine is displaced from tubulin with a compound that does not fluoresce when bound to tubulin, the displacement is measured as a decrease in fluorescence. Podophyllotoxin and CA-4 competed with colchicine for binding on tubulin and caused a decrease in the fluorescence of the colchicine-tubulin complex. Podophyllotoxin (20  $\mu\text{M}$ ) inhibited fluorescence by 98% and 20  $\mu\text{M}$  CA-4 inhibited fluorescence by 87% (Fig. 4C). Polygamain (5  $\mu\text{M}$ ) was able to inhibit fluorescence by 21%, and 20  $\mu\text{M}$  polygamain was able to inhibit fluorescence by 80% (Fig. 4C). These data indicate that polygamain competes with colchicine binding to purified tubulin, suggesting that polygamain binds to tubulin within the colchicine binding site.

**Molecular Modeling of Polygamain in the Colchicine Site.** Molecular docking studies were conducted to explore the interaction between tubulin and polygamain, and how it differs from podophyllotoxin. The majority of polygamain poses generated by the docking studies produced conformations similar to that of podophyllotoxin. We also found that the vast majority of low-energy trajectory conformations generated by the molecular dynamics very closely approximated podophyllotoxin (Protein Data Bank code 1SA1).

Analyses of the molecular dynamics simulations generated 25 lowest-energy minima of the polygamain-docked model revealed a similar pattern of interactions and spatial positioning that is likely to be due to its intrinsic rigidity. The interactions and the three-dimensional arrangement of polygamain occupy a space similar to that of podophyllotoxin (Fig. 5). The polygamain benzodioxole moiety is buried well inside the hydrophobic pocket containing Val238, Cys241, Leu242, Leu248, Ala250, Leu255, Ala317, Val318, and Ala354 of  $\beta$ -tubulin [residue numbering as described previously by Ravelli et al. (2004)] and forms favorable hydrophobic interactions similar to those of podophyllotoxin above and below the plane of the phenyl ring. The dimethoxyphenyl moiety in podophyllotoxin forms an H-bond with Cys- $\beta$ 241, and the methyl groups of the trimethoxyphenyl moiety are oriented so that favorable hydrophobic interactions occur with the side chains of  $\beta$ -tubulin residues Val238, Leu242, Leu248, Ala250, Leu255, Ala317, Val318, and Ala354 located above and below the plane of the phenyl ring. This interaction provides significant differences with respect to the interaction of polygamain and podophyllotoxin with tubulin.

**Aqueous Solubility.** The aqueous solubility of polygamain was determined and compared with the solubility of CA-4 and podophyllotoxin (Table 2). The results show that CA-4 is soluble in a universal aqueous buffer up to 399  $\mu\text{M}$  and podophyllotoxin is soluble up to 428  $\mu\text{M}$ . Polygamain shows lower aqueous solubility of 78  $\mu\text{M}$ .

## Discussion

The identification of polygamain as a new tubulin-binding antimetabolic agent demonstrates that higher plants remain a source for the discovery of new microtubule active agents. Polygamain has cellular activities similar to other microtubule-depolymerizing agents in that it causes a dose-dependent loss of cellular microtubules and the formation of aberrant mitotic spindles that are ineffective in aligning the chromosomes at the metaphase plate, leading ultimately to  $G_2/M$  arrest. Polygamain does not seem to have any phenotypic effects on mitotic spindles or interphase microtubules to

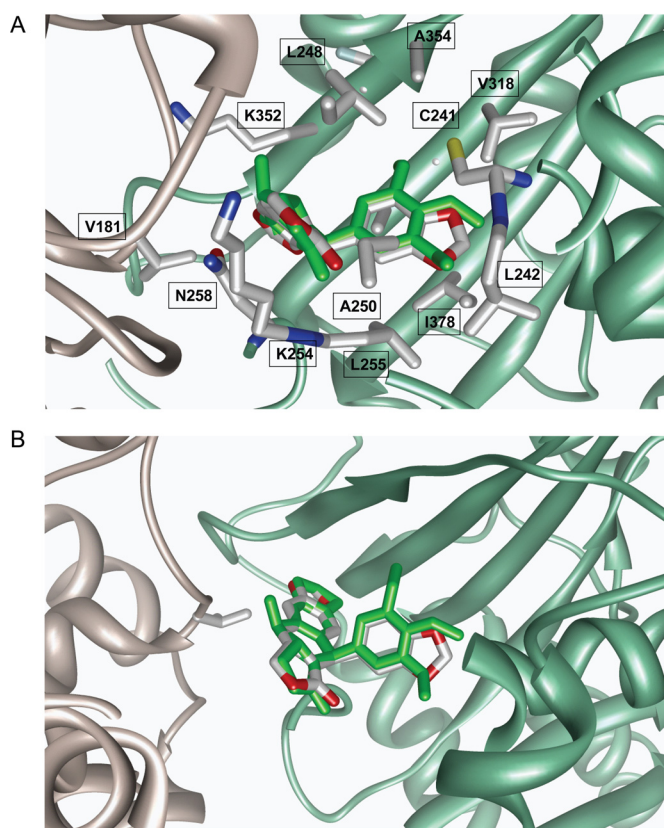


**Fig. 5.** Structural model of polygamain in complex with  $\alpha$ -tubulin (gray) and  $\beta$ -tubulin (green). A, polygamain (red and gray) structural model with podophyllotoxin (green) overlaid onto it. The polypeptide backbones are rendered as ribbons. Interactive residue side chains on tubulin are shown in stick model. B, root-mean-square fit of polygamain (red and gray) with podophyllotoxin (green) inside the colchicine-binding site.  $\alpha$ , $\beta$ -Tubulin is represented by the gray and green ribbon, respectively.

TABLE 2

Aqueous solubility of polygamain, podophyllotoxin, and CA-4

Compound	Aqueous Solubility
	$\mu\text{M}$
Polygamain	78 $\pm$ 0.1
Podophyllotoxin	428 $\pm$ 13.2
CA-4	399 $\pm$ 9.1

differentiate it from other microtubule-destabilizing agents. However, differences between polygamain, CA-4, and podophyllotoxin are seen when comparing the ratio of the anti-proliferative and microtubule depolymerizing effects. We have used the ratio of microtubule depolymerizing potency to antiproliferative potency ( $EC_{50}/IC_{50}$  ratio) to compare a large number of colchicine site agents for mechanistic similarities and potential differences (Lee et al., 2010; Gangjee et al., 2011; Risinger et al., 2011). Podophyllotoxin has an  $EC_{50}/IC_{50}$  ratio of 1, CA-4 has a ratio of 4, and polygamain has a substantially higher ratio of 11, suggesting subtle differences among these compounds. It is also interesting to note that podophyllotoxin, with the lowest ratio, has no clinical utility, whereas CA-4, with a higher ratio, is currently in stage III clinical trials. A ratio of 5.4 was obtained with 2-methoxyestradiol (Rao et al., 2002), and although it did not advance to US Food and Drug Administration approval for cancer, it was devoid of serious side effects (James et al., 2007). This ratio may not only relate mechanistic differences and binding

modes but also the differential activity in cancer versus normal cells. This is further supported by the low cytotoxicity of polygamain and CA-4 in normal epithelial cells compared with podophyllotoxin, which caused substantial cytotoxicity. In future in vivo studies, it will be interesting to determine whether this relationship can predict toxicity. The low yield of polygamain from *A. madrensis* plants precluded in vivo studies, but synthetic approaches are being developed to address this important question in the future.

Polygamain is less potent in cancer cells than CA-4 or podophyllotoxin, with an average  $IC_{50}$  of 52.7 nM compared with average  $IC_{50}$  values of 5.5 and 10.6 nM for CA-4 and podophyllotoxin, respectively. In contrast to the potency rank of the antiproliferative effects of polygamain, CA-4, and podophyllotoxin against cancer cells, in the tubulin polymerization assays, polygamain and podophyllotoxin were essentially equipotent and were more potent than CA-4. The different isotype composition of brain-derived tubulin used in the biochemical assay compared with the tubulin isotypes expressed in epithelial-derived cancer cells may underlie this difference in relative potency. Brain tissue is enriched in the  $\beta$ II and  $\beta$ III tubulin isotypes, which account for 58 and 25% of neuronal tubulin, respectively (Panda et al., 1994). It is possible that polygamain has higher affinity for  $\beta$ II tubulin compared with CA-4. The expression of  $\beta$ III tubulin in the HeLa-derived WT $\beta$ III cells had no effect on the potency of any of these compounds compared with the parental cells, suggesting that  $\beta$ III tubulin in brain tubulin does not contribute to differences in potency among these agents.

Our studies indicated several differences between the binding modes of polygamain and podophyllotoxin. Colchicine site binding agents are traditionally believed to need a biaryl structure, limited conformational mobility, and a trimethoxyphenyl group to effectively bind this site (Xu et al., 2009). For purposes of this discussion, the rings of podophyllotoxin will be labeled from left to right (Fig. 1), with the lactone designated as ring A. Modeling studies indicate podophyllotoxin contains six pharmacophore fragments that bind within this site. These pharmacophore fragments include two H-bond acceptors, the methoxy group on ring C and the ester on ring D; one H-bond donor, the OH group on ring C; two hydrophobic centers, the A ring lactone and the E ring trimethoxyphenyl; and one planar group, ring B (Nguyen et al., 2005). The absence of the OH group on ring C of polygamain precludes interactions with  $\alpha$ -tubulin because of a loss of this H-bond donor. Podophyllotoxin is able to interact with the carbonyl oxygen of Thr $\alpha$ 179 through its OH on ring C (Nguyen et al., 2005). Polygamain can no longer form that interaction, translating to fewer favorable interactions. The second, more important difference is the lack of methoxy groups in polygamain. Podophyllotoxin has three methoxy groups on the E ring that act as H-bond acceptors. The methoxy group on C-4, where numbering begins with the carbon bonded to ring C (Fig. 1), acts as an H-bond acceptor leading to a stabilizing interaction with the sulfur of Cys $\beta$ 241. In polygamain, the entire trimethoxyphenyl ring of podophyllotoxin is replaced with a benzodioxole moiety. The lactone ring portion of this moiety is still a hydrophobic center and an H-bond acceptor, but the favorable interactions formed with Cys $\beta$ 241 are now highly unlikely because they would need to form with an ethyl group. Fewer favorable interactions may be responsible for the lower potency of

polygamain in cellular assays compared with podophyllotoxin. It is interesting to note that Cys $\beta$ 241 is the same residue that differs between  $\beta$ III and other  $\beta$ -tubulin isotypes. Our data suggest that the interactions of the drugs with this specific residue are not critical, because no differences were noted among the drugs with regard to relative resistance in the parental and  $\beta$ III expressing HeLa cells.

Polygamain contains structural similarities to podophyllotoxin and other colchicine site-binding agents and yet has features that distinguish it. The three methoxy groups on podophyllotoxin allow a much larger degree of flexibility compared with polygamain, which has a rigid structure (Casnovas et al., 2005). The flexibility of podophyllotoxin allows a one-step but completely reversible reaction with tubulin. This interaction has a high entropic penalty because the residues within the colchicine binding pocket must undergo a conformational change to accommodate binding (Cortese et al., 1977; Torin Huzil et al., 2006). The rigidity seen in polygamain may lead to a more entropically favorable binding reaction. Colchicine is also a very rigid molecule, and colchicine binding proceeds in a slow, two-step reaction that is essentially irreversible (Cortese et al., 1977). Polygamain may have a binding mode more like that of colchicine, contributing to its high cellular persistence in the clonogenic assay.

Interesting differences were noted among these compounds in the cellular persistence measured using a washout clonogenic assay. Both CA-4 and polygamain had substantially higher cellular persistence compared with podophyllotoxin. Factors that can contribute to cellular persistence include the ability of a drug to be concentrated across the cell membrane and the rate of intracellular metabolism (Towle et al., 2011). Major differences in cellular persistence are found among microtubule targeted agents. Colchicine, vinblastine, eribulin, and taccalonolide A have excellent persistence after washout, whereas paclitaxel and vinblastine do not (Risinger and Mooberry, 2011; Towle et al., 2011). One might expect that enhanced cellular persistence might be associated with more neurotoxicity, but this has not proven to be the case with eribulin (Wozniak et al., 2011). Cellular persistence can be useful for comparing drug analogs for in vivo testing, but cellular persistence alone cannot predict optimal antitumor response. Many other factors relate to in vivo efficacy, including half-life, volume of distribution, and metabolism.

The probable binding interaction of polygamain within the colchicine site of tubulin offers new opportunities for structural modifications that may generate analogs with higher affinity and the potential for lower toxicity. Additional modification of polygamain, however, will be needed to facilitate optimal aqueous solubility for in vivo testing.

The identification of polygamain as a new microtubule depolymerizer provides a new pharmacophore for binding within the colchicine site. Polygamain's unique orientation within this site, potent activity, and good cellular persistence provides a new modeling platform for analog development for the design and synthesis of improved colchicine site agents. The synthesis of polygamain analogs with improved aqueous solubility that retain fewer hydrophobic interactions within the binding site has the potential to reduce the toxicities associated with the essentially irreversible binding that occurs with colchicine and the strong interactions of podophyllotoxin. A new binding mode together with notable cellular

persistence provides a new approach to identify colchicine site agents that can improve on those found in nature for optimal antitumor activities and clinical potential.

#### Acknowledgments

We thank Dr. April Risinger and Cristina Rohena for thoughtful comments and editing assistance and Lauren Clarke for assistance in the original plant collection and processing.

#### Authorship Contributions

*Participated in research design:* Hartley, Peng, Brown, and Mooberry.

*Conducted experiments:* Hartley, Peng, Fest, and Dakshanamurthy.

*Contributed new reagents or analytic tools:* Peng and Frantz.

*Performed data analysis:* Hartley, Peng, Dakshanamurthy, Frantz, Brown, and Mooberry.

*Wrote or contributed to the writing of this manuscript:* Hartley, Peng, Dakshanamurthy, Brown, and Mooberry.

#### References

- Banerjee A and Ludueña RF (1992) Kinetics of colchicine binding to purified beta-tubulin isotypes from bovine brain. *J Biol Chem* **267**:13335–13339.
- Bayly CI, Cieplak P, Cornell WD, and Kollman PA (1993) A well-behaved electrostatic potential based method using charge restraints for deriving atomic charges—the RESP model. *J Phys Chem* **97**:10269–10280.
- Bhattacharyya B and Wolff J (1974) Promotion of fluorescence upon binding of colchicine to tubulin. *Proc Natl Acad Sci USA* **71**:2627–2631.
- Blagosklonny MV, Darzynkiewicz Z, Halicka HD, Pozarowski P, Demidenko ZN, Barry JJ, Kamath KR, and Herrmann RA (2004) Paclitaxel induces primary and postmitotic G1 arrest in human arterial smooth muscle cells. *Cell Cycle* **3**:1050–1056.
- Boyd MR and Paull KD (1995) Some practical considerations and applications of the national cancer institute in vitro anticancer drug discovery screen. *Drug Dev Res* **34**:91–109.
- Casanovas J, Namba AM, da Silva R, and Alemán C (2005) DFT-GIAO study of aryltetralin lignan lactones: conformational analyses and chemical shifts calculations. *Bioorg Chem* **33**:484–492.
- Cortese F, Bhattacharyya B, and Wolff J (1977) Podophyllotoxin as a probe for the colchicine binding site of tubulin. *J Biol Chem* **252**:1134–1140.
- Das L, Gupta S, Dasgupta D, Poddar A, Janik ME, and Bhattacharyya B (2009) Binding of indanocine to the colchicine site on tubulin promotes fluorescence, and its binding parameters resemble those of the colchicine analogue AC. *Biochemistry* **48**:1628–1635.
- Dumontet C and Jordan MA (2010) Microtubule-binding agents: a dynamic field of cancer therapeutics. *Nat Rev Drug Discov* **9**:790–803.
- Dumontet C, Jordan MA, and Lee FF (2009) Ixabepilone: targeting betaIII-tubulin expression in taxane-resistant malignancies. *Mol Cancer Ther* **8**:17–25.
- Eigsti OJ and Dustin P (1955) *Colchicine—in Agriculture, Medicine, Biology, and Chemistry*. Iowa State College Press, Ames, IA.
- Galmarini CM, Treilleux I, Cardoso F, Bernard-Marty C, Durbecq V, Gancberg D, Bissery MC, Paesmans M, Larsimont D, Piccart MJ, et al. (2008) Class III beta-tubulin isotype predicts response in advanced breast cancer patients randomly treated either with single-agent doxorubicin or docetaxel. *Clin Cancer Res* **14**:4511–4516.
- Gangjee A, Zhao Y, Hamel E, Westbrook C, and Mooberry SL (2011) Synthesis and biological activities of (R)- and (S)-N-(4-methoxyphenyl)-N,2,6-trimethyl-6,7-dihydro-5H-cyclopenta[d]pyrimidin-4-aminium chloride as potent cytotoxic anti-tubulin agents. *J Med Chem* **54**:6151–6155.
- Gottesman MM, Fojo T, and Bates SE (2002) Multidrug resistance in cancer: role of ATP-dependent transporters. *Nat Rev Cancer* **2**:48–58.
- Hokanson GC (1979) Lignans of polygala-polygama (polygalaceae)-deoxy-podophyllotoxin and 3 new lignan lactones. *J Nat Prod* **42**:378–384.
- Huang HC, Shi J, Orth JD, and Mitchison TJ (2009) Evidence that mitotic exit is a better cancer therapeutic target than spindle assembly. *Cancer Cell* **16**:347–358.
- James J, Murry DJ, Treston AM, Storniolo AM, Sledge GW, Sidor C, and Miller KD (2007) Phase I safety, pharmacokinetic and pharmacodynamic studies of 2-methoxyestradiol alone or in combination with docetaxel in patients with locally recurrent or metastatic breast cancer. *Invest New Drugs* **25**:41–48.
- Kavallaris M (2010) Microtubules and resistance to tubulin-binding agents. *Nat Rev Cancer* **10**:194–204.
- Krishan A (1975) Rapid flow cytofluorometric analysis of mammalian cell cycle by propidium iodide staining. *J Cell Biol* **66**:188–193.
- Lee L, Robb LM, Lee M, Davis R, Mackay H, Chavda S, Babu B, O'Brien EL, Risinger AL, Mooberry SL, et al. (2010) Design, synthesis, and biological evaluations of 2,5-diaryl-2,3-dihydro-1,3,4-oxadiazoline analogs of combretastatin-A4. *J Med Chem* **53**:325–334.
- Ludueña RF (1998) Multiple forms of tubulin: different gene products and covalent modifications. *Int Rev Cytol* **178**:207–275.
- Ludueña RF and Banerjee A (2008) The isotypes of tubulin, in *The Role of Microtubule in Cell Biology, Neurobiology, and Oncology* (Fojo T ed), Humana Press, Totowa, NJ.
- Mooberry SL, Tien G, Hernandez AH, Plubrukarn A, and Davidson BS (1999) Laulimalide and isolaulimalide, new paclitaxel-like microtubule-stabilizing agents. *Cancer Res* **59**:653–660.
- Nguyen TL, McGrath C, Hermone AR, Burnett JC, Zaharevitz DW, Day BW, Wipf P, Hamel E, and Gussio R (2005) A common pharmacophore for a diverse set of colchicine site inhibitors using a structure-based approach. *J Med Chem* **48**:6107–6116.
- Noble RL, Beer CT, and Cutts JH (1958) Role of chance observations in chemotherapy: *Vinca rosea*. *Ann NY Acad Sci* **76**:882–894.
- Panda D, Miller HP, Banerjee A, Ludueña RF, and Wilson L (1994) Microtubule dynamics in vitro are regulated by the tubulin isotype composition. *Proc Natl Acad Sci USA* **91**:11358–11362.
- Penson RT, Oliva E, Skates SJ, Glyptis T, Fuller AF Jr, Goodman A, and Seiden MV (2004) Expression of multidrug resistance-1 protein inversely correlates with paclitaxel response and survival in ovarian cancer patients: a study in serial samples. *Gynecol Oncol* **93**:98–106.
- Pettit GR, Cragg GM, and Singh SB (1987) Antineoplastic agents, 122. Constituents of *Combretum caffrum*. *J Nat Prod* **50**:386–391.
- Pettit GR, Temple C Jr, Narayanan VL, Varma R, Simpson MJ, Boyd MR, Renner GA, and Bansal N (1995) Antineoplastic agents 322. Synthesis of combretastatin A-4 prodrugs. *Anticancer Drug Des* **10**:299–309.
- Podwysotszki V (1880) *Pharmakologische Studien über Podophyllum peltatum. Arbeiten aus dem pharmakologischem Institut der Universität Dorpat* **16**:29–52.
- Rao PN, Cessac JW, Tinley TL, and Mooberry SL (2002) Synthesis and antimetabolic activity of novel 2-methoxyestradiol analogs. *Steroids* **67**:1079–1089.
- Ravelli RB, Gigant B, Curmi PA, Jourdain I, Lachkar S, Sobel A, and Knossow M (2004) Insight into tubulin regulation from a complex with colchicine and a stathmin-like domain. *Nature* **428**:198–202.
- Risinger AL, Jackson EM, Polin LA, Helms GL, LeBoeuf DA, Joe PA, Hopper-Borge E, Ludueña RF, Kruh GD, and Mooberry SL (2008) The taccalonolides: microtubule stabilizers that circumvent clinically relevant taxane resistance mechanisms. *Cancer Res* **68**:8881–8888.
- Risinger AL and Mooberry SL (2011) Cellular studies reveal mechanistic differences between taccalonolide A and paclitaxel. *Cell Cycle* **10**:2162–2171.
- Risinger AL, Westbrook CD, Encinas A, Mülbaier M, Schultes CM, Wawro S, Lewis JD, Janssen B, Giles FJ, and Mooberry SL (2011) ELR510444, a novel microtubule disruptor with multiple mechanisms of action. *J Pharmacol Exp Ther* **336**:652–660.
- Sève P, Reiman T, and Dumontet C (2010) The role of betaIII tubulin in predicting chemoresistance in non-small cell lung cancer. *Lung Cancer* **67**:136–143.
- Sheriha GM, Abouamer K, Elshatawi BZ, Ashour AS, Abed FA, and Alhallaou HH (1987) Quinoline alkaloids and cytotoxic lignans from haplophyllum-tuberculatum. *Phytochemistry* **26**:3339–3341.
- Skehan P, Storeng R, Scudiero D, Monks A, McMahon J, Vistica D, Warren JT, Bokesch H, Kenney S, and Boyd MR (1990) New colorimetric cytotoxicity assay for anticancer-drug screening. *J Natl Cancer Inst* **82**:1107–1112.
- Smith CD, Zhang X, Mooberry SL, Patterson GM, and Moore RE (1994) Cryptophycin: a new antimicrotubule agent active against drug-resistant cells. *Cancer Res* **54**:3779–3784.
- Tinley TL, Leal RM, Randall-Hlubek DA, Cessac JW, Wilkens LR, Rao PN, and Mooberry SL (2003a) Novel 2-methoxyestradiol analogues with antitumor activity. *Cancer Res* **63**:1538–1549.
- Tinley TL, Randall-Hlubek DA, Leal RM, Jackson EM, Cessac JW, Quada JC Jr, Hemscheidt TK, and Mooberry SL (2003b) Taccalonolides E and A: plant-derived steroids with microtubule-stabilizing activity. *Cancer Res* **63**:3211–3220.
- Torin Huzil J, Ludueña RF, and Tuszynski J (2006) Comparative modelling of human  $\beta$  tubulin isotypes and implications for drug binding. *Nanotechnology* **17**:S90–S100.
- Towle MJ, Salvato KA, Wels BF, Aalfs KK, Zheng W, Seletsky BM, Zhu X, Lewis BM, Kishi Y, Yu MJ, et al. (2011) Eribulin induces irreversible mitotic blockade: implications of cell-based pharmacodynamics for in vivo efficacy under intermittent dosing conditions. *Cancer Res* **71**:496–505.
- Wang J, Wolf RM, Caldwell JW, Kollman PA, and Case DA (2004) Development and testing of a general amber force field. *J Comput Chem* **25**:1157–1174.
- Wani MC, Taylor HL, Wall ME, Coggon P, and McPhail AT (1971) Plant antitumor agents. VI. The isolation and structure of Taxol, a novel antileukemic and antitumor agent from *Taxus brevifolia*. *J Am Chem Soc* **93**:2325–2327.
- Wozniak KM, Nomoto K, Lapidus RG, Wu Y, Carozzi V, Cavaletti G, Hayakawa K, Hosokawa S, Towle MJ, Littlefield BA, et al. (2011) Comparison of neuropathy-inducing effects of eribulin mesylate, paclitaxel, and ixabepilone in mice. *Cancer Res* **71**:3952–3962.
- Xu H, Lv M, and Tian X (2009) A review on hemisynthesis, biosynthesis, biological activities, mode of action, and structure-activity relationship of podophyllotoxins: 2003–2007. *Curr Med Chem* **16**:327–349.
- Yeh JJ, Hsu WH, Wang JJ, Ho ST, and Kao A (2003) Predicting chemotherapy response to paclitaxel-based therapy in advanced non-small-cell lung cancer with P-glycoprotein expression. *Respiration* **70**:32–35.

**Address correspondence to:** Dr. Susan L. Mooberry, University of Texas Health Science Center at San Antonio, 7703 Floyd Curl Drive, San Antonio, TX 78229. E-mail: mooberry@uthscsa.edu